Chemical Science International Journal

22(4): 1-10, 2018; Article no.CSIJ.41169
ISSN: 2456-706X
(Past name: American Chemical Science Journal, Past ISSN: 2249-0205)

Isotherm and Kinetic Studies on the Adsorptive Removal of Metanil Yellow and Neutral Red Dyes Using Copper Oxide Nanoparticles

Muhammad Adamu Ibrahim[1*] and Muhammad Bashir Ibrahim[1]

[1]Department of Pure and Industrial Chemistry, Bayero University, P.M.B. 3011, Kano, Nigeria.

Authors' contributions

This work was carried out in collaboration between both authors. Author MAI is a postgraduate research student under the supervision of author MBI. Both authors read and approved the final manuscript.

Article Information

DOI: 10.9734/CSJI/2018/41169
Editor(s):
(1) Nagatoshi Nishiwaki, Professor, Kochi University of Technology, Japan.
Reviewers:
(1) Tsamo Cornelius, University of Maroua, Cameroon.
(2) Atiya Firdous, Karachi University, Pakistan.
(3) Muhammad Raziq Rahimi Kooh, Universiti Brunei Darussalam, Brunei.
Complete Peer review History: http://www.sciencedomain.org/review-history/24635

Original Research Article

Received 24th February 2018
Accepted 9th May 2018
Published 16th May 2018

ABSTRACT

This study investigated the adsorption property of copper oxide nanoparticles (CuO-NPs) for the removal of Metanil Yellow (MY) and Neutral Red (NR). The influence of variables such as contact time, initial concentration and pH for the adsorption process were investigated. The percentage removal and optimum contact time for the removal of MY and NR were obtained as 70.7% during 25 min and 56.9% over 30 min respectively. The experimental isotherms data were analyzed using Langmuir, Temkin, Freundlich and Dubinin-Radushkevich (D-R) isotherms and it was observed that MY fits closely to Temkin isotherm with an R^2 value of 0.860 and NR fits more to D-R isotherm with R^2 0.953. The kinetics of both MY and NR dyes fits better to pseudo-second order with the experimental values of q_e 2.844 and 3.536 for NR and MY respectively been closer to the calculated values of the q_e 2.739 and 3.222 for NR and MY respectively. Effect of pH of both dyes shows that they adsorb better at the initial pH of 3.37 and 5.09 for NR and MY respectively. Lower values of mean square energies of 0.354 for NR and 0.791 kJ/mol for MY indicates that the adsorption process is physical. The results indicated that copper oxide nanoparticle can be used as a low-cost adsorbent for the removal of MY and NR from aqueous solutions.

**Corresponding author: E-mail: mibrahim042@gmail.com; mbibrahim.chm@buk.edu.ng*

Keywords: Adsorption; nanoparticles; isotherms; kinetics; metanil yellow; neutral red.

1. INTRODUCTION

With increasing development in technology, the world is reaching to new horizons. Among the consequences of rapid growth are environmental disorders and pollution problems. Besides other needs, the demand of water for industries has increased rapidly and resulted in the generation of a large amount of wastewater containing a large number of pollutants. Dyes are an important class of industrial pollutants [1,2]. Dyes are kind of organic compound with a complex aromatic molecular structure that can bring a bright and firm colour to other materials. Also, the complex aromatic molecular structures of dyes make them stable and difficult to biodegrade [3]. Textile industries consume large quantities of water and chemicals, especially in dyeing and finishing processes. On average, 60–90% of total water consumption is spent in washing processes [4]. This research is based on Neutral red which is a cationic dye and Metanil yellow which is an Azo dye. Neutral red is a cationic dye used extensively for nuclear counterstaining in biological research. It is also widely used in analytical laboratories as pH indicator. The toxic nature of the dye can be explained by considering the fact that on decomposition it gives out hazardous products, such as carbon monoxide (CO), carbon dioxide (CO_2), nitrogen oxides and hydrogen chlorides [5]. The neutral red dye is a toxic dye, which has generally been removed from water samples through the use of sand [6], nanoparticle Fe_3O_4 [7] and modified historic [8]. Amongst several dyes, azo dyes constitute an important class of synthetic, coloured, organic compounds, which are categorized by the presence of one or more azo bonds (–N=N–). Especially azo dyes which contribute to about 60% of all used dyes are difficult to degrade due to their complex structure and synthetic nature [9]. They are toxic, sometimes generate aesthetic problems and have been reported for possible mutagenic and carcinogenic effects [10]. It also affects photosynthetic activity in the water body. Further, degradation of these dyes leads to the formation of toxic amines [11]. Therefore, the removal of these coloured compounds from effluent turns out to be significant before they enter the environment.

Performance of adsorption process using metal oxide nanoparticles for wastewater treatment containing heavy metals in a laboratory scale reactor was assessed by Taman et al. [12]. Copper oxide nano-particles were prepared and fully characterized considering their adsorption properties (surface area and pore size distribution) as well as their chemical structure and morphology. Taman et al. [12] carried out a research study using copper oxide nanoparticles to adsorb Cd^{2+} and Fe^{3+} which showed good potential for the removal of MY and NR. The selectivity order of the adsorbent is Fe^{3+}>Cd^{2+}. From these results, it can be concluded that the CuO nanoparticles is a promising adsorbent for the removal of heavy metals from aqueous solutions. In this research, CuO nano particle was used as an adsorbent for the removal of NR and MY dyes with kinetic and isotherm studies, characterization of the adsorbent both before and after as well as optimization of different parameters being carried out.

2. MATERIALS AND METHODS

2.1 Synthesis of Copper Oxide Nanoparticles

The method employed by Mayekar et al. [13] was adopted for the synthesis of the Copper oxide nanoparticle with the use of Polyethylene glycol (PEG) instead of polyvinylpyrrolidone (PVP) which plays the same role to stabilize the aggregation of the metal ion. For the synthesis of copper oxide nanoparticles, 7.68 g of copper nitrate trihydrate ($Cu(NO_3)_2.3H_2O$) was mixed with 2.4 g of polyethene glycol (PEG) and 200 ml of distilled water. The solution was stirred using magnetic stirrer and heated until it reaches 60ºC. 1.0 M of sodium hydroxide solution and 1.0 M hydrochloric acid were used to adjust the pH of the solution to 7.0 (Neutral). Sodium hydroxide solution was added drop by drop followed by heating and stirring for two hours. The brownish-black precipitate was formed [14]. It was centrifuged and oven dried at 50ºC for eight hours to get copper oxide nanopowder. The FTIR of the nanoparticle both before and after adsorption was conducted.

2.2 Batch Adsorption Experiment

The influence of variables such as pH, contact time and initial dye concentration on the adsorptive removal of dyes were all investigated in batch mode. In each experiment, 100 mL of dye solution in a 120 mL bottle was agitated and stirred at 300 rpm along with a fixed mass of the nanoparticles at an initial concentration of 10 mg/L, initial pH of the dyes and at a

constant temperature of 30 ± 2ºC. The mixture was then centrifuged and the residual concentrations of the dyes were determined spectrophotometrically using UV-Visible spectrophotometer (Model Hitachi 2800) at a corresponding λ_{max} of each dye; 430 nm and 455 nm for MY (70 %, Merck) and NR (90 %, Merck) respectively. 1.43 g and 1.11 g of MY and NR were dissolved in 1000 ml of distilled water to prepare the standard solution. The obtained experimental data at various times and concentration were fitted to different models to evaluate and calculate the kinetics and isotherm parameters. The solution pH was adjusted by the addition of dilute aqueous solutions of HCl and NaOH (0.1 M).

The removal efficiency and adsorption capacity of the adsorbent were calculated from equations (1) and (2) respectively:

$$R(\%) = \frac{(C_0 - C_t)}{C_0} \times 100 \quad (1)$$

$$q_e = \frac{(C_0 - C_t)V}{m} \quad (2)$$

Where C_0 (mg/L) is the initial dye concentration, C_e (mg/L) is the equilibrium dye concentration, m (g) is the adsorbent mass, and V (L) is the volume of the dye solution.

The results obtained were subjected to equilibrium, kinetics and adsorption isotherm studies.

2.3 Adsorption Isotherms

The linear form of Langmuir isotherm is expressed as in equation (3):

$$\frac{C_e}{q_e} = \frac{1}{K_{LQm}} + \frac{C_e}{Q_m} \quad (3)$$

Where C_e is the equilibrium concentration (mg L^{-1}), q_e is the amount of adsorbed dye at equilibrium (mg g^{-1}), Q_m is the maximum adsorption capacity which represents monolayer coverage (mg g^{-1}) , K_L is the Langmuir isotherm constant related to the energy of adsorption (L mg-1). The values of K_L and Q_m can be determined from the slope and intercept of the linear plot of C_e/q_e versus C_e . The nature of the adsorption process is explained by the dimensionless parameter R_L defined by equation (4) which could be either unfavourable (R_L > 1), linear (R_L = 1), favourable (0 < R_L < 1), or irreversible (R_L = 0) [15-17].

$$R_L = \frac{1}{(1+K_L C_O)} \quad (4)$$

where C_o is the initial dye concentration and K_L is Langmuir constant.

A linear form of the Freundlich equation is generally expressed by equation (5):

$$\log qe = \log K_f + \frac{1}{n_f} \log Ce \quad (5)$$

where qe is the amount of adsorbed dye at equilibrium (mg/g), Ce is the equilibrium concentration of the adsorbate (mg/L), K_F is the Freundlich adsorption constant related to adsorption capacity of the adsorbent (mg/g), and $1/n_F$ is the adsorption intensity. The values of K_F and $1/n_F$ were calculated from the intercept and slope of the plot of log qe versus log Ce [15,18].

The linear form of Temkin isotherm is expressed as in equation (6):

$$q_e = B_T \ln A_T + B_T \ln Ce \quad (6)$$

Where B_T is the Temkin constant related to the heat of adsorption and A_T is the equilibrium binding constant (L mg-1). The constants A_T and B_T can be determined by a plot of q_e versus ln C_e with B_T defined by equation (7):

$$B_T = RT/b_T \quad (7)$$

b_T = Temkin isotherm constant; *R* = universal gas constant (8.314 J/mol/K); *T* = Temperature at 298 K.

Dubnin - Radushkevich (D-R) isotherm was applied in order to distinguish between physical and chemical adsorptions through adsorption energies. The D-R equation has the form defined by equation (8):

$$\ln q_e = \ln(X_m) - \beta\varepsilon^2 \quad (8)$$

Xm (mg/g) is the theoretical monolayer saturation capacity, β (mol^2/kJ^2) is the activity coefficient related to the mean free energy of adsorption per mole of the adsorbate when it is transferred from infinity in the solution to the surface of the solid and ε (J/mol) is Polanyi potential defined by equation (9):

$$\varepsilon = RT \ln (1 + 1/Ce) \quad (9)$$

where R is gas constant (R = 8.314 J/(mol · K)) and T is temperature (K). The mean free energy E (kJ/mol) is calculated using the relationship.

$$E = \sqrt{\frac{1}{2\beta}} \quad (10)$$

The plot of lnqe against ε^2 yield the slope β (mol^2/kJ^2) and the intercept yields the adsorption capacity Xm (mg/g) [19].

2.4 Adsorption Kinetics

Pseudo first order integrated rate equation can be represented in a linear form as in equation (11):

$$\ln (q_e - q_t) = \ln q_e - K t \quad (11)$$

where qe is the equilibrium adsorption capacity (mg/g), qt is the mass of dyes adsorbed at time t (mg/g), k is the first order rate constant (min^{-1}) [20].

Pseudo-second order integrated rate equation is defined by equation (12):

$$\frac{t}{q_t} = \frac{1}{k_2 q_e^2} + \frac{1}{q_e} t \quad (12)$$

A plot of $\frac{t}{q_t}$ versus t should give a slope and intercept of $\frac{1}{q_e}$ and $\frac{1}{k_2 q_e^2}$ giving a linear relationship for the applicability of the second order kinetics [21,22].

The Elovich equation generally used is expressed by equation (13):

$$q_t = \frac{1}{\beta} \ln (t) + \frac{1}{\beta} \ln (\alpha \beta) \quad (13)$$

q_t was plotted against ln(t). α is the initial adsorption rate (mg $g^{-1}min^{-1}$) and *β* is the desorption constant (g mg^{-1}) which are obtained from the slope and intercept of the plot [23].

Intraparticle diffusion is the most commonly used technique for identifying the mechanism involved in the sorption process by fitting the experimental data in an intraparticle diffusion plot. Previous studies by various researchers showed that the plot of q_t *versus* $t^{0.5}$ represents multi linearity, which characterizes the two or more steps involved in the sorption process [24].

$$q_t = k_{diff} t^{1/2} + C \quad (14)$$

Where *C* is the intercept and k_{diff} is the intraparticle diffusion rate constant ($mgg^{-1}min^{-1/2}$) from the plot of *qt* versus $t^{1/2}$ [25].

3. RESULTS AND DISCUSSION

3.1 Effect of Contact Time

The increase in contact time at 300 rpm stirring rate leads to enhancement in the dye adsorption. The adsorption of MY appears a fast process, so about 70.7% of the dye removal took place within the first 25 min using initial dye concentration of 10 mg/L, (Fig. 1) which is due to high interaction between adsorbent and the dye, and also the availability of more active sites on the nanoparticles for the dye adsorption. The amounts of adsorption reached a limiting value beyond which no significant improvement is observed. This is because all active sites for further adsorption have been occupied by the molecules. Therefore, the equilibrium adsorption occurred at about 25 min; this time was considered as the equilibrium time in kinetic studies. This adsorption process shows lower percentage removal at a higher time when compared to that of Muthuraja and Kannan [26], which reported 85% removal after 20 minutes using initial dye concentration of 100 mg/L in their work for kinetic and isotherm studies of metanil yellow dye on mesoporous aluminophosphate molecular sieves. This difference might be attributed to the fact that higher dosage and concentration was used in their research and also the difference in the adsorbent used. However, the effect of contact time on the adsorption of NR dye has an equilibrium attained after 30 minutes with maximum removal percentage of about 56.9%. This is slow when compared to 98% removal Neutral red dye from water samples using adsorption on baggasse and sawdust as reported by Elhami et al. [27] after the first 30 minutes as well. This may be due to the fact that higher concentration (100 mg/L) was used by Elhami et al. [27] than 10 mg/L used in the determination of the contact time.

3.2 Adsorption Kinetics

From Table 1 the q_e experimental and the q_e calculated values from the pseudo first order are very far from each other for MY and NR dyes. The calculated correlation coefficients (R^2) for the two dyes were very low when compared with that of other kinetic models in the table. This shows that the adsorptions of MY and NR onto CuO-NP do not follow the pseudo first-order kinetics. The q_e experimental and the ag_e calculated values from the pseudo-second-order kinetic model for the dyes are very close to each

other. The calculated correlation coefficients (R^2) were also close to unity for pseudo-second-order kinetic than the other tested kinetic models. Therefore, the adsorption can be approximated more appropriately by pseudo-second-order kinetic model for all the studied adsorbates as was supported by Sumanjit et al. [28]. The rate constant of pseudo-second order adsorption (k_2) obtained for NR was found to be lower than those computed for MY (Table 1). A phenomenon like this according to Kalalagh et al. [29] indicates that the uptake of NR onto CuO-NP from aqueous solution was more rapid and favourable.

According to Sumanjit et al. [28] the chemical significance for Elovich constants α and β has not been clearly resolved. However, for both dyes β > α suggesting desorption process to be more prominent than adsorption and there may be a link to the low values of R^2 (Table 1). In intraparticle diffusion, adsorption process occurs as a three steps process. The first step involves the transport of the dyes molecules from the bulk solution onto the external surface of CuO-NP by diffusion through the boundary layer. The second step is the diffusion of the dye molecules from the external surface into the pores of the CuO-NP adsorbent. The last step is the final equilibrium stage, where the dye molecules were adsorbed on the active sites on the internal surface of the pore, and the intra-particle diffusion plot starts slowing down due to the solute concentration getting lower in the solution [30]. If these lines pass through the origin then intraparticle diffusion is the rate-controlling step [31]. When the plots do not pass through the origin, this is indicative of some degree of boundary layer control and these further shows that the intraparticle diffusion is not the only rate-limiting step, but also other kinetic models may control the rate of the adsorption, all of which may be operating simultaneously [31]. For the two plots, the line did not pass through the origin showing that intra particle diffusion was not the only rate limiting step. The intercept of the plot indicates the boundary layer effect [30]. Therefore, both surface adsorption and intra-particle diffusion mechanisms were simultaneously operating in the adsorption behaviours using the CuO-NP adsorbent.

3.3 Effect of Initial Concentration

The effect of initial concentration of MY and NR on their removal efficiency by CuO-NPs adsorbent for the concentration of 10, 20, 30, 40, 50, 100, 150, 200, 250 mg/L was studied and respective results were shown in Fig. 2. The optimum concentration for adsorption of MY and NR onto CuO-NPs are 100 and 200 mg/L respectively. From Fig. 2, the removal of NR and MY dyes were found to be increasing up to the region of higher concentration and this can be due to the availability of active sites for saturation at higher concentration and also can be due to a substrate having a high affinity for MY than NR. These results agreed with the results obtained by Muthuraja and Kannan [26].

3.4 Adsorption Isotherm

In Langmuir isotherm, the nature of the adsorption process could be either unfavourable (R_L > 1), linear (R_L = 1), favourable (0 < R_L < 1), or irreversible (R_L = 0) [16]. The value of R_L of 0.046 for MY which is less than 1, shows that the adsorption process is favourable [32]. The experimental data from Table 2 showed that the adsorption process for NR did not fit to the

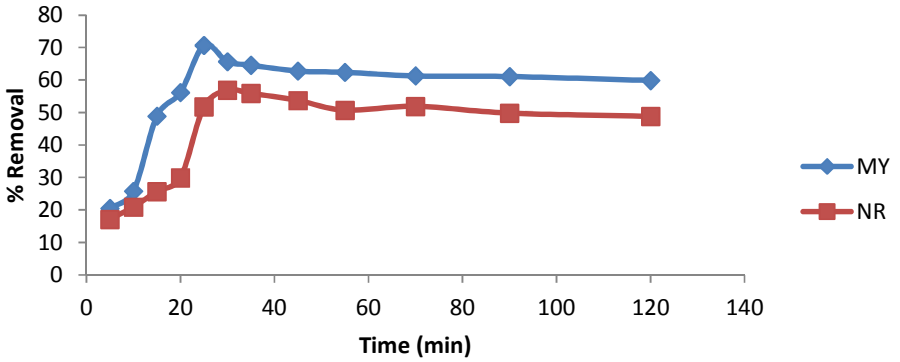

Fig. 1. Effect of contact time on the removal of MY and NR dyes at an initial concentration of 10 mg/L, at room temperature and at initial pH

Table 1. Kinetics parameters for adsorption of NR and MY on CuO-NPs

Models	Kinetic parameters	NR	MY
	$q_{e,exp.}$(mg/g)	2.844	3.536
Pseudo First Order	$q_{e,cal.}$(mg/g)	1.192	1.007
	k_1(min^{-1})	0.016	0.010
	R^2	0.410	0.234
Pseudo Second Order	$q_{e,cal.}$(mg/g)	2.739	3.222
	k_2(g/mg.min)	0.052	0.073
	R^2	0.942	0.979
Elovich	α(mg/g.min)	0.598	1.484
	β(g/mg)	1.576	1.551
	R^2	0.638	0.575
Intraparticle Diffusion	C (mg/g)	0.954	1.624
	k_{diff}(mg/g.$min^{-1/2}$)	0.195	0.185
	R^2	0.474	0.373

Conditions: (C_o = 10mg/L, m = 0.2 g, T= 303K)

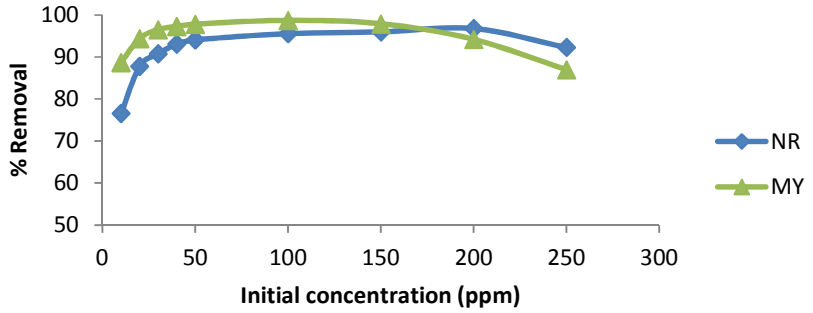

Fig. 2. Effect of initial dye concentration on the removal of NR and MY

Langmuir isotherm, giving negative slopes and intercepts, leading to the conclusion that the adsorption behavior of NR does not follow the assumption on which the Langmuir approach is based, as such it does not fit Langmuir isotherm [33-35]. The value of K_L for adsorption of MY onto CuO-NPs is indicating high bond strength between MY and CuO-NPs [36].

It was reported that Freundlich isotherm constant o_f, can be used to explore the favourability of the adsorption process. The adsorption process is said to be favourable when the value of n_F satisfies the condition 1 < n_F <10, otherwise it becomes unfavourable [35]. The value of n_f MY is within the range 1 < n_F <10, indicating the adsorption is favourable, while that of NR is not within the range as shown in the Table 2, indicating the adsorption is not favourable. The K_f value for adsorption of MY is higher with 31.688 mg/g indicating it have the highest adsorption capacity on CuO-NPs [33].

For Temkin isotherm, the values of A_T 1.973 and 0.517 for MY and NR respectively shows that NR has lower adsorption potential or binding potential to the Nanoparticles [29]. The temkin heat of adsorption B_T values of 57.48 J/mol for MY and 28.64 J/mol for NR being less than 80 kJ/mol indicates a favourable physical adsorption for all the dyes as described by Inglezakis and Zorpas [37]. The R^2 value for the adsorption of MY is higher than that of other models, this shows that adsorption of MY onto CuO-NP fits closely to Temkin isotherm.

From D-R isotherm, the magnitude of E is used to estimate the type of adsorption mechanism. If the magnitude of E is between 8 and 16 kJ/mol, it is indicative of chemical adsorption, while for the value of E < 8 kJ/mol; the adsorption process is physical adsorption [38]. The values of mean square energy E of 0.791 kJ/mol for MY and 0.354 kJ/mol for NR both being < 8 kJ/mol indicates a successful physical adsorption. The difference of Q_m derived from Langmuir and X_m derived from D-R model may be attributed to the different definition of maximum capacity in the two models. In Langmuir model, Q_m represents the maximum adsorption of dye at monolayer

coverage, but in D-R model X_m represents the maximum adsorption of dye molecules at the total specific micropores volume of the adsorbent [38]. Hence, the values show that adsorption takes place more in the micropores or pores than on the surface of the adsorbent. The R^2 value for the adsorption of NR is higher than that of other models, this shows that Adsorption of NR onto CuO-NP fits better with D-R isotherm.

3.5 Effect of pH

The initial pH value of the solution is one of the most important factors influencing dye adsorption. This is because the pH value determines the number of hydrogen ions capable of competing with the positively charged dye ions for the active sites on the adsorbent. In this research, the pH of the dyes was varied from 2 to 12 MY, for NR pH was varied from 2 to 7 to avoid precipitation of the dye [39], but for research purpose pH range of 2-12 was also taken to study the effects. The initial pH of all the dyes were measured and adsorption was carried out for the initial pH values. Initial pH for MY and NR measured are 5.09 and 3.37 respectively. Effect of pH on the removal of MY and NR is shown in Figs. 3 and 4 respectively. For MY, there is an increase in pH (from 2 to 5.09) which causes the adsorption to increase from 67.4 to 98.7 %, then decreases to 66.4 % at pH 12. For NR, there is an increase in adsorption (from pH 2-3.37) increasing the adsorption from 82.1 to 96.8 %. The adsorption decreases to 91.3 % at pH 8. It further increases to 96.1 % at pH10 and decreases to 95.8 % at pH 12. The sudden increase in removal at pH10 is due to the combined effect of precipitation and adsorption of the dye. The effect of precipitation was observed at ranges of pH 8-12. This result is in agreement with the findings of Nejati et al. [40] in the Adsorption of Metanil yellow azoic dye from aqueous solution onto Mg-Fe-NO_3 layered double hydroxide which shows the same pattern of the result as the findings of this research.

3.6 Fourier Transform- Infrared (FT-IR) Characterization

The type and net charge of functional groups bonded to the CuO-NPs surface are important in understanding the mechanism of adsorption of ionic adsorbates on the substrate [41]. FT-IR spectra of CuO-NPs and after adsorption with MY and NR were taken and compared with the CuO-NPs before adsorption to obtain information on the nature of the possible adsorbent-dye molecules interactions. The spectrum of the samples shows the presence of several functional groups (-OH, C≡C, C=C, C-H). The FT-IR spectra of the CuO-NPs both before and after adsorption with MY and NR were shown in Table 3. This demonstrates that after the adsorption the shifting occurs both to higher and lower wave numbers. This shifting indicated that there were binding processes, taking place on the surface of the substrate. Broad band of 3200-3550 cm^{-1} represented –OH groups, 2850-3000 cm^{-1} represented aliphatic C-H group, 2100-2250 cm^{-1} represented C≡C group. The functional groups could act as a chemical of binding agents where hydroxyl group dissociate negatively charged active surface [41].

Table 2. Adsorption isotherms parameters for adsorption of NR and MY on CuO-NPs

Adsorption isotherm	Parameters	MY	NR
Langmuir	K_L(L mg^{-1})	0.084	-0.031
	R_L	0.046	-0.15
	Q_M(mg/g)	312.5	-67.57
	R^2	0.474	0.056
Temkin	A_T(L/mg)	1.973	0.519
	b_T	43.10	86.50
	B_T(J/mol)	57.48	28.64
	R^2	0.860	0.908
Freundlich	n_f	1.506	0.697
	k_f(mg/g)	31.69	1.722
	R^2	0.578	0.717
D-R	X_M(mg/g)	216.1	72.06
	E(kJ/mol)	0.791	0.354
	R^2	0.701	0.953

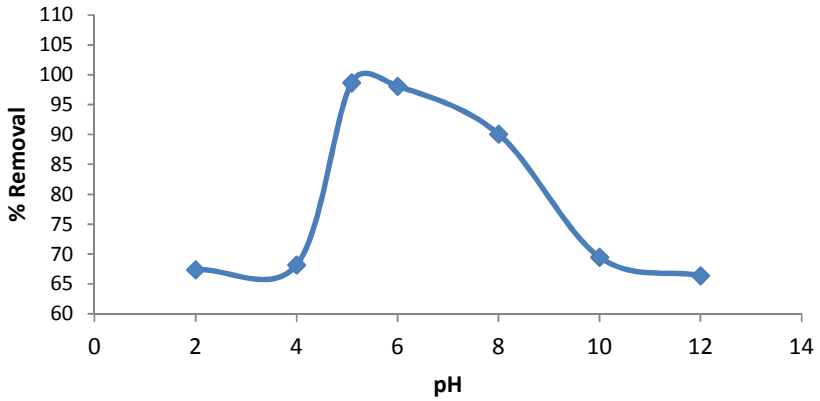

Fig. 3. Effect of pH on the removal of MY at an initial dye concentration of 100 mg/L and room temperature

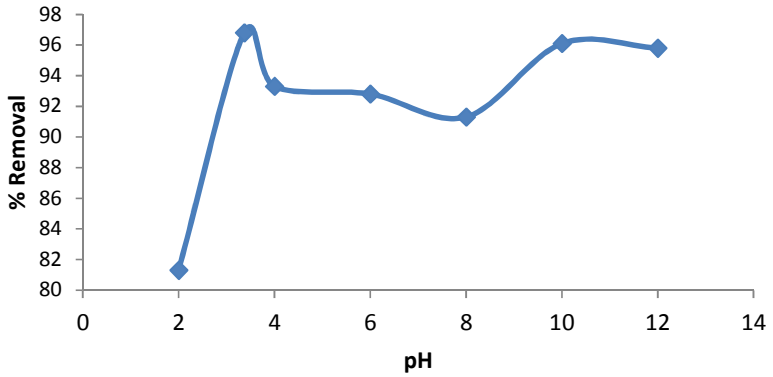

Fig. 4. Effect of pH on the removal of NR at an initial dye concentration of 200 mg/L and room temperature

Table 3. Summary of FT-IR results of CuO-NPs both before and after adsorption with MY and NR

Peak	CuO-NPs before Adsorption	After adsorption with MY	After adsorption with NR	Assignment
1	3420	3402 +18	3417 +3	Bonded –OH
2	2880	2925 - 45	2929 -49	Aliphatic C-H group
3	2199	2110 +89	2113 +86	C≡C group
4	1599	1592 +7	1603 -4	C=C stretching
5	1350	1328 +22	1346 +4	-OH bending
6	1097	1037 + 60	1063 +34	C-O stretching

4. CONCLUSION

In this research, copper oxide nanoparticle has been synthesized and used as an effective adsorbent for the removal of MY and NR dye from aqueous solutions. The effects of variables, such as initial dye concentration, contact time and pH were studied on the adsorption. Isotherm modelling revealed that the Temkin equation described the adsorption of MY and D-R describe the adsorption of NR. All the dyes fit successfully to pseudo-second-order kinetic model. The values of mean free energy indicate the adsorption of all the dyes to be physical in nature. FTIR result showed increase intensities which indicates that there is an interaction between the adsorbent and the dye molecules. In view of these results, it can be

concluded that synthesized CuO-NP can be utilized as a low-cost and effective adsorbent in the removal of MY and NR from aqueous solutions.

COMPETING INTERESTS

Authors have declared that no competing interests exist.

REFERENCES

1. Aksu Z. Biosorption of reactive dyes by dried activated sludge: Equilibrium and kinetic modelling. Biochem. Eng. J. 2001;7: 79–84.
2. Aksu Z. Application of biosorption for the removal of organic pollutants: A review. Process Biochem. 2005;40:997–1026.
3. Chang MW, Chung CC, Chern JM, Chen TS. Dye decomposition kinetics by UV/H2O2: Initial rate analysis by effective kinetic modelling methodology. Chem. Eng. Sci. 2010;65:135–140.
4. Daneshvar N, Sorkhabi HA, Kasiri MB. Decolorization of dye solution containing acid red 14 by electrocoagulation with a comparative investigation of different electrode connections. J. Hazard. Mater. 2004;112:55–62.
5. Irama M, Guo C, Guan Y, Ishfaq A, Li H. Adsorption and magnetic removal of neutral red dye from aqueous solution using Fe3O4 hollow nanospheres. Journal of Hazardous Materials. 2010;81:1039-1050.
6. Rauf MA, Shehadi IA, Hassan WW. Dyes and Pigments. 2007;75:723.
7. Iram M, Guo Ch, Guan Y, Ishfaq A, Liu H. Journal of Hazardous Material. 2010;181: 1039.
8. Yue D, Jing Y, Ma J, Xia Ch, Yin X, Jia Y. Desalination. 2011;267:9.
9. Fu F, Viraraghavan T. Fungal decolorization of dye wastewaters: A review. Bioresource Technol. 2001;79: 251–62.
10. Chang J, Chou C, Lin Y, Lin P, Ho J, Hu TL. Kinetic characteristics of bacterial azo-dye decolorization by pseudomonas luteola. Water Res. 2001;35:2841–50.
11. Chung KT, Fulk GE, Egan M. Reduction of azo dyes in intestinal anerobes. Appl. Environ. Microbiol. 1978;35:558–562.
12. Taman R, Ossman ME, Mansour MS, Farag HA. Metal oxide nano-particles as an adsorbent for removal of heavy metals. Journal of Advanced Chemical Engineering. 2015;5:125:1-8.
13. Mayekar J, Dhar V, Radha S. Synthesis of copper oxide nanoparticles using simple chemical route. International Journal of Scientific & Engineering Research. 2014; 10(5):928-930.
14. Singh J, Kaur G, Rawat M. A brief review on synthesis and characterization of copper oxide nanoparticles and its applications. Journal of Bioelectronics and Nanotechnology. 2016;1(1):9.
15. Karimi H, Mousavi S, Sadeghian B. Silver nanoparticle loaded on activated carbon as efficient adsorbent for removal of methyl orange. Indian Journal of Science and Technology. 2012;5(3):2346-2353.
16. Asl MN, Mahmodi NM, Teymouri P, Shahmoradi B, Rezaee R, Maleki A. Adsorption of organic dyes using copper oxide nanoparticles: Isotherm and kinetic studies. Desalination and Water Treatment. 2016;1–10.
17. Langmuir I. The constitution and fundamental properties of solids and liquids. Journal of the American Chemical Society. 1916;38:2221-2295.
18. Freundlich HMF. Over the adsorption in solution. Journal of Physical Chemistry. 1906;57:385-471.
19. Dubinin MM, Radushkevich LV. Equation of the characteristic curve of activated charcoal. Proceedings of the National Academy of Sciences. 1947;55:327.
20. Lagergren S. About the theory of so called adsorption of soluble substances, Kungliga Svenska Vetenskapsakademiens Handlingar. 1898;24:1-39.
21. Thilagan J, Gopalakrishnan S, Kannadasan T. Adsorption of copper (II) ions in aqueous solution by *Chitosan immobilised* on red soil: Isotherms, kinetics and mechanism. International journal of pharmaceutical and chemical sciences. 2013;2(2):1055-1066.
22. Ho YS, McKay G. Sorption of dye from aqueous solution by peat, Chem. Eng. J. 1998;70:115-124.
23. Gok O, Ozcan A, Erdem BA, Ozcan S. Prediction of the kinetics, equilibrium and thermodynamic parameters of adsorption of copper(II) ions onto 8-hydroxy quinolone immobilized bentonite. Colloids and Surfaces A: Physicochem. Eng. Aspects. 2008;31:174–185.
24. Ramuthai S, Nandhakumar V, Thiruchel M, Arivoli S, Vijayakumaran V. Rhodamine B

adsorption-kinetic, mechanistic and thermodynamic studies. E-Journal of Chemistry. 2009;6(S1):S363-S373.
25. Weber W, Morris J. Kinetics of adsorption on carbon from solution, J. Sanit. Eng. Div. 1963;89:31-60.
26. Muthuraja K, Kannan C. Kinetic and Isotherm Studies of Removal of Metanil Yellow Dye on Mesoporous Aluminophosphate Molecular Sieves. Chemical Science Transactions. 2013; 2(S1):S195-S201.
27. Elhami S, Faraji H, Taheri M. Removal of neutral red dye from water samples using adsorption on bagasse and sawdust, J. Chem. Soc. Pak. 2012;34(2):269-273.
28. Sumanjit Rani S, Mahajan RK. Equilibrium, kinetics and thermodynamic parameters for adsorptive removal of dye Basic Blue 9 by ground nut shells and Eichhornia. Arabian Journal of Chemistry. 2012;1-14.
29. Kalalagh SS, Babazadeh H, Nazemi AH, Manshouri M. Isotherm and kinetic studies on adsorption of Pb, Zn and Cu by Kaolinite. Caspian J. Env. Sci. 2011;9(2): 243-255.
30. Nuengmatcha P, Mahachai R, Chanthai S. Adsorption capacity of the as-synthetic graphene oxide for the removal of alizarin red s dye from aqueous solution. Orient. J. Chem. 2016;32(3):1399-1410.
31. Ozcan A, Ozcan AS, Tunali S, Akar T, Kiran I. Determination of the equilibrium, kinetic and thermodynamic parameters of adsorption of copper(II) ions onto seeds of *Capsicum annuum.* Journal of Hazardous Materials. 2005;B124:200–208.
32. Sampranpiboon P, Charnkeitkong P, Feng X. Equilibrium isotherm models for adsorption of zinc (II) ion from aqueous solution on pulp waste. Wseas Transactions on Environment and Development. 2014;10:35-48.
33. Kiurski J, Adamovic S, Krstic J, Oros I, Miloradov MV. Adsorption efficiency of low-cost materials in the removal of Zn(II) ions from printing developers. Bulletin of Engineering Tome IV. 2011;61-66.
34. Kiurski J, Adamović S, Oros I, Krstić J, Kovačević I. Adsorption feasibility in the Cr (total) ions removal from waste printing developer. Global NEST Journal. 2012; 14(1):18-23.
35. Ibrahim MB, Sani S. Comparative isotherms studies on adsorptive removal of congo red from wastewater by watermelon rinds and neem-tree leaves. Open Journal of Physical Chemistry. 2014;4:139-146.
36. Erhayem M, Al-Tohami F, Mohamed R, Ahmida K. Isotherm, kinetic and thermodynamic studies for the sorption of mercury (II) onto activated carbon from *Rosmarinus officinalis* Leaves. American Journal of Analytical Chemistry. 2015;6:1-10.
37. Inglezakis VJ, Zorpas AA. Heat of adsorption, adsorption energy and activation energy in adsorption and ion exchange systems. Desalination and Water Treatment. 2012;39:149–157.
38. El-Araby HA, Ibrahim AMA, Mangood AH, Abdel-Rahman AAH. Sesame husk as adsorbent for copper (II) ions removal from aqueous solution. Journal of Geoscience and Environment Protection. 2017;5:109-152.
39. Gong R, Li Mei, Yang C, Sun Y, Chen J. Removal of cationic dyes from aqueous solution by adsorption on peanut hull. Journal of hazardous materials. 2005; B121:247-250.
40. Nejati K, Rezvani Z, Mansurfar M, Mirzaee A, Mahkam M. Adsorption of metanil yellow azoic dye from aqueous solution onto Mg-Fe-NO3 layered double hydroxide. Z. Anorg. Allg. Chem. 2011; 637:1573–1579.
41. Nale BY, Kagbu JA, Uzairu A, Nwankwere ET, Saidu S, Musa H. Kinetic and equilibrium studies of the adsorption of lead(II) and nickel(II) ions from aqueous solutions on activated carbon prepared from maize cob. Der Chemica Sinica. 2012;3(2):302-312.

Peer-review history:
The peer review history for this paper can be accessed here:
http://www.sciencedomain.org/review-history/24635